Synthesis and Properties of Nb-containing Mesoporous Materials with Bimodal Pores Using TEOS and Layered Perovskite K_2NbO_3F

Masataka Ogasawara, Sumio Kato, Hiroshi Tsukidate, Takahiro Akaogi, Yoshio Moriya, and Shinichi Nakata*
Faculty of Engineering and Resource Science, Akita University, 1-1 Tegatagakuen-machi, Akita, 010-8502

(Received November 19, 2004; CL-041397)

We synthesized Si–Nb-mesoporous materials using TEOS, layered perovskite K_2NbO_3F, and HDTMACl as starting materials. TEM-EDX and IR spectra measurements indicated that niobium was introduced in the silica framework, forming Si–O–Nb bond. Mesopores due to the templating effect of HDTMA formed in the nanoparticle, thus producing a bimodal mesoporous material.

Mesoporous materials synthesized using structure-directing agent (SDA) such as long-chain surfactant are expected to find applications in catalysts and absorbents because they have ordered pores with uniform size of 2–50 nm and high specific surface area.[1] Such a material is particularly promising for dealing with nanosize molecules. Mesoporous nanoparticles have large pores due to the presence of interparticle spaces, resulting in formation of bimodal porous material. This has the advantage of reducing transport limitations. Several synthesis methods have been reported for preparing bimodal mesopores, such as the method using two kinds of surfactants[2] and others.[3,4]

Many researches on catalytic activity of mesoporous materials containing transitional metal have been performed. Mesoporous materials containing niobium in the pore wall have been investigated regarding catalytic activity for oxidation[5,6] and hydrodesulfurization.[7] Generally, Nb-mesoporous materials are synthesized using niobium chloride[6,7] or niobium ethoxide[8,9] solution as a starting material. Recently, we discovered that mesostructured materials were formed from layered perovskite K_2NbO_3F and alkyltrimethylammonium chloride.[10] This result suggests that layered material K_2NbO_3F is useful as a starting material for a mesoporous material. However, in the case of synthesis from K_2NbO_3F and hexadecyltrimethylammonium chloride (HDTMACl), the mesostructure collapsed by calcination at 603 K. Synthesis of mesoporous materials containing Si–Nb complex oxide in the pore wall was examined from the viewpoint of improving stability. In this study, we succeeded in preparing Si–Nb-mesoporous oxides with bimodal pores from K_2NbO_3F and TEOS and investigated their microstructures and properties.

HDTMACl was used as the SDA. $x\,\mathrm{cm}^3$ ($x = 1, 2, 4$) of TEOS and 24 cm^3 of 0.1 $\mathrm{mol/dm}^3$ aqueous HDTMACl solution were added to 50 cm^3 of distilled water. 0.56 g of powder K_2NbO_3F was immediately dispersed in this solution. The suspension was stirred with a magnetic stirrer at 323 K for 3 h. The resulting white precipitate was recovered by filtration and drying. The dried samples were calcined in air at 753 K for 3 h in order to remove SDA. Structural characterization of the products was performed using powder X-ray diffraction (XRD) and infrared spectroscopy (IR). The pore and particle shapes were observed by transmission electron microscopy (TEM) and Si/Nb ratio was determined by energy dispersive X-ray analysis (EDX). N_2 adsorption–desorption isotherms were recorded at 77 K and the surface area was obtained from Brunauer–Emmett–Teller (BET) plot. The pore size distribution and pore volume were estimated by the Dollimore–Heal method.

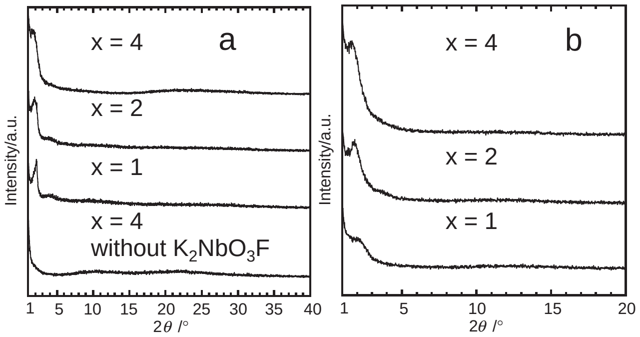

Figure 1. XRD patterns of as–synthesized (left) and calcined (right) products.

The XRD patterns of as-synthesized products for three different TEOS additions, $x = 1, 2$, and $4\,\mathrm{cm}^3$, and a product synthesized without K_2NbO_3F are shown in Figure 1a. The diffraction peaks of the products for $x = 1$ and 2 were indexed on the basis of 2-D-hexagonal type mesostructure. For $x = 4$, only one peak was observed at d spacing of 5.0 nm. This peak also indicates formation of mesostructure. In the case of the product synthesized at 323 K for 3 h using 4 cm^3 TEOS without K_2NbO_3F, no XRD peak indicating formation of mesostructure was observed. This result suggests that the presence of the K_2NbO_3F induces the formation of the mesostructure.

The XRD patterns of calcined products are shown in Figure 1b. For $x = 2$ and 4, apparent diffraction peaks were observed in the range $2\theta = 1.5$–$2°$, while the peak for $x = 1$ was broad. These results indicate that the periodicity of the mesostructure remained after removal of SDA for $x = 2$ and 4. In the case of $x = 1$, however, the periodicity decreased with removal of SDA. The IR spectra of calcined products are shown in Figure 2. All the products exhibit a symmetric stretching vibration band at around 810 cm^{-1} and an antisymmetric vibration band at around 1080 cm^{-1} of the tetrahedral $SiO_4{}^{4-}$ structural units. A peak at around 960 cm^{-1} was also observed, which was used to examine the incorporation of transition metal in the silica framework.[11,12] From the fact that this peak has been observed in Nb-mesoporous silicas,[7,13,14] it is considered that the products have Si–O–Nb bond in the framework.

The TEM images of calcined products for $x = 1$ and 4 are shown in Figure 3. Both of the products have 2–3 nm diameter pores due to the templating effect of HDTMA. However, the pore arrangement was not uniform but wormhole like. Addition-

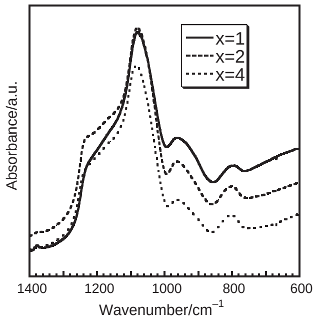

Figure 2. IR spectra of calcined products dispersed in KBr pellets.

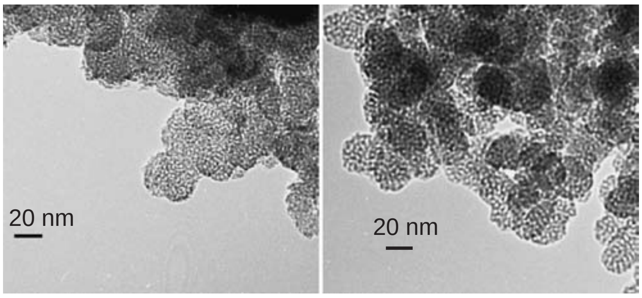

Figure 3. TEM image of the calcined products for $x = 1$ (left) and 4 (right).

ally, for $x = 4$, ca. 20–30 nm diameter nanosize particle including mesopores was formed. Si/Nb ratios estimated by EDX in the meoporous materials for $x = 1$ and 4 were 12 and 61, respectively, indicating introduction of Nb into the silica framework.

The nitrogen adsorption–desorption isotherms of products are shown Figure 4a. The amount of nitrogen adsorption for $x = 1$ is evidently lower than for $x = 2$ and 4. This result is related to decrease of the mesostructure periodicity observed by XRD measurement. In the case of products at $x = 2$ and 4, two-step increases in nitrogen adsorption were observed in the ranges of $0.2 < P/P_0 < 0.4$ and $P/P_0 > 0.85$. This behavior indicates that the mesoporous materials have bimodal pores. The pore size distribution, pore diameter and BET surface area are shown Figure 4b and Table 1. For $x = 4$, two peaks in pore size distribution were observed at around 2–3 and 15–40 nm. From the results of TEM observation, it is considered that the small pores of around 2–3 nm are due to templating effect of HDTMA and the large pores of around 15–40 nm are due to interpaticle spaces among the nanoparticles.

In summary, we synthesized mesoporous material from TEOS, layered perovskite K_2NbO_3F and HDTMACl. TEM–EDX and IR spectra measurements indicated that niobium was introduced in the silica framework, resulting in formation of Si–O–Nb bond. In the case of the synthesis without K_2NbO_3F, mesostructure was not formed. Therefore, it is considered that K_2NbO_3F induces the formation of the mesostructure. In addition, for $x = 4$, we found that nanosize particle including mesopores formed. The Si–Nb-mesoporous material with bimodal pores prepared in this study is a promising material for catalyst dealing with nano scale compounds such as biomolecules. Research into the details of the formation mechanism and application studies are in progress.

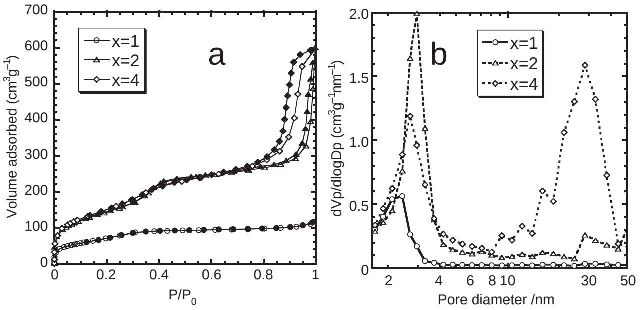

Figure 4. N_2 adsorption–desorption isotherms (left) and pore size distribution (right) of calcined products.

Table 1. Physical properties of calcined products

Amount of TEOS x/cm^3	S_{BET} /m^{2}g^{-1}	Pore diameter /nm		Pore volume /cm^{3}g^{-1}
1	261	2.1	—	0.16
2	527	2.9	—	0.79
4	561	2.7	28.3	0.91

This work was supported in part by Grant-in-Aid for Encouragement of Young Scientists the Ministry of Education, Culture, Sports, Science and Technology of Japan (No.15760573).

References

1 T. Yanagisawa, T. Shimizu, K. Kuroda, and C. Kato, *Bull. Chem. Soc. Jpn.*, **63**, 988 (1990).
2 K. Suzuki, K. Ikari, and H. Imai, *J. Am. Chem. Soc.*, **126**, 462 (2004).
3 J. El Haskouri, D. O. de Zárate, C. Guillem, J. Latorre, M. Caldés, A. Beltrán, D. Beltrán, A. B. Descalzo, G. Rodríguez-López, R. Martínez-Máñez, M. D. Marcos, and P. Amorós, *Chem. Commun.*, **2002**, 330.
4 J. El Haskouri, D. O. de Zárate, C. Guillem, A. Beltrán-Porter, M. Caldés, M. D. Marcos, D. Beltrán-Porter, J. Latorre, and P. Amorós, *Chem. Mater.*, **14**, 4502 (2002).
5 M. Zioleka, A. Lewandowskaa, B. Grzybowskab, and A. Klisińska, *React. Kinet. Catal. Lett.*, **80**, 199 (2003).
6 N. K. Mal and M. Fujiwara, *Chem. Commun.*, **2002**, 2702.
7 P. Yang, D. Zhao, D. I. Margolese, B. F. Chmelka, and G. D. Stucky, *Nature*, **396**, 152 (1998).
8 L. Cedeño, D. Hernandez, T. Klimova, and J. Ramirez, *Appl. Catal., A*, **217**, 39 (2003).
9 D. M. Antonelli and J. Y. Ying, *Angew. Chem., Int. Ed. Engl.*, **35**, 426 (1996).
10 M. Ogasawara, S. Kato, H. Tsukidate, T. Akaogi, Y. Moriya, and S. Nakata, *Chem. Lett.*, **33**, 1138 (2004).
11 A. Corma, M. T. Navarro, and J. P. Pariente, *J. Chem. Soc., Chem. Commun.*, **1994**, 147.
12 Z. Fu, J. Chen, D. Yin, D. Yin, L. Zhang, and Y. Zhang, *Catal. Lett.*, **66**, 105 (2000).
13 Y. Liu, K. Murata, and M. Inaba, *Chem. Lett.*, **32**, 992 (2003).
14 V. Parvulescu, C. Constantin, and B. L. Su, *J. Mol. Catal. A: Chem.*, **202**, 171 (2003).

Published on the web (Advance View) January 15, 2005; DOI 10.1246/cl.2005.208